How to cite: *Angew. Chem. Int. Ed.* **2021**, *60*, 13317–13322
International Edition: doi.org/10.1002/anie.202017057
German Edition: doi.org/10.1002/ange.202017057

Supercapacitors **Hot Paper**

Electrochemical Characterization of Single Layer Graphene/Electrolyte Interface: Effect of Solvent on the Interfacial Capacitance

Yih-Chyng Wu[+], Jianglin Ye[+], Gengping Jiang, Kun Ni, Na Shu, Pierre-Louis Taberna, Yanwu Zhu, and Patrice Simon**

Abstract: *The development of the basic understanding of the charge storage mechanisms in electrodes for energy storage applications needs deep characterization of the electrode/electrolyte interface. In this work, we studied the charge of the double layer capacitance at single layer graphene (SLG) electrode used as a model material, in neat (EMIm-TFSI) and solvated (with acetonitrile) ionic liquid electrodes. The combination of electrochemical impedance spectroscopy and gravimetric electrochemical quartz crystal microbalance (EQCM) measurements evidence that the presence of solvent drastically increases the charge carrier density at the SLG/ionic liquid interface. The capacitance is thus governed not only by the electronic properties of the graphene, but also by the specific organization of the electrolyte side at the SLG surface originating from the strong interactions existing between the $EMIm^+$ cations and SLG surface. EQCM measurements also show that the carbon structure, with the presence of sp^2 carbons, affects the charge storage mechanism by favoring counter-ion adsorption on SLG electrode versus ion exchange mechanism in amorphous porous carbons.*

Introduction

Nowadays, energy storage is one important aspect of portable products. Electrochemical double layer capacitors (EDLCs), known as supercapacitors, can offer high power output and long cycle life when compared to batteries.[1] Among all future candidates, graphene-based materials are promising for EDLC electrode because of their superior properties, such as high conductivity, electrochemical stability and controllable porosity.[2]

Graphene is defined as a two-dimensional sheet of carbon atoms arranged in a honeycomb network, which endows it a high theoretical surface of $2630\,m^2\,g^{-1}$ and a theoretical capacity up to $550\,F\,g^{-1}$ under certain conditions.[3] Such a high capacitance may be achieved when resolving the restacking issue appearing in multilayer graphene film electrode,[4] as the normalized capacitance per area decays with the number of layers in the stacking.[5] To this end, single layer graphene (SLG) offers a good platform as a model material for studying the ion adsorption and fluxes on the carbon surface, while keeping the high surface area of intrinsic graphene at least for one side.[6] Several works have reported a V-shaped capacitance versus a wide-range of applied potential (C-V) for SLG, where the minimum capacitance is located around the Dirac point and the total capacitance increases linearly with gate potential.[7] The existence of a quantum capacitance (C_Q), related to the number of available charge carriers in the graphene,[7a,8] has been proposed to explain such a V-shape signature where C_Q largely restricts the total interfacial capacitance (C_{int}) of SLG, expressed as $1/C_{int} = 1/C_H + 1/C_Q$ with C_H being the Helmholtz capacitance. Based on the standard band theory calculation, as the number of graphene layers increases, the quantum capacitance increases, which may result in the interfacial capacitance (C_{int}) less dependent on the potential for multilayer graphene-based materials.[9]

On the other hand, the nature and concentration of electrolytes are critical aspects in determining the electrochemical double layer (EDL) at the electrode surface.[9c] Experiments have shown the shape of C-V plots of silver (Ag) electrode has a transition from camel-like to U-like one when moving from pure ionic liquid (IL) to diluted electrolyte (< 2 molarity), in agreement with the mean-field model where the short-range ion correlations have to be taken into consideration.[10] Back to graphene, our previous work using electrochemical quartz crystal microbalance (EQCM) has also evidenced the specific ion fluxes and separation at the

[*] Y.-C. Wu,[+] P.-L. Taberna, P. Simon
Université Paul Sabatier, CIRIMAT UMR CNRS 5085
118 route de Narbonne, 31062 Toulouse (France)
and
Réseau sur le Stockage Electrochimique de l'Energie (RS2E), FR CNRS 3459 (France)
E-mail: simon@chimie.ups-tlse.fr
J. Ye,[+] K. Ni, N. Shu, Y. Zhu
Hefei National Research Center for Physical Sciences at the Microscale, & CAS Key Laboratory of Materials for Energy Conversion, & Department of Materials Science and Engineering, & iChEM, University of Science and Technology of China
Hefei, Anhui 230026 (China)
E-mail: zhuyanwu@ustc.edu.cn
G. Jiang
College of Science, Wuhan University of Science and Technology
Wuhan 430080 (China)
[+] These authors contributed equally to this work.
Supporting information and the ORCID identification number(s) for the author(s) of this article can be found under https://doi.org/10.1002/anie.202017057.

SLG surface immersed in neat ionic liquid electrolyte.[11] In addition, a series of simulations have established the models which include the contribution of C_H and C_D (diffuse layer capacitance) to describe the experimental results of SLG in aqueous electrolytes.[12] It was found that the interfacial capacitance of polarized SLG electrodes changes with the degree of ion packing (the total number of anions and cations in the electrolyte bulk divided by total number of available sites at the electrode surface), ion-ion interaction (through a correlation length parameter) and size of ions in neat ionic liquids.[13] For instance, when the ion packing factor is high, C_Q would control the interfacial capacitance near the potential of zero charge (pzc) without seeing the effect of ion-ion correlation, resulting in a camel-shape dependence of the total capacitance on the applied potential. However, the simulation only considered ion-ion interactions in the electrolyte but not interactions between ions and polarized SLG, which may significantly influence the electrochemical behavior of SLG as well. It was shown, for instance, that the adsorption of alkyl imidazolium cations causes n-type doping of graphene and the magnitude of doping increases with cation alkyl chain length.[14]

The interfacial capacitance, especially in concentrated electrolytes, is very sensitive not only to the electronic structure of the electrode, but also to the nature of the electrolytes at the polarized interface.[13,15] Unfortunately, the experimental approaches aiming at understanding the correlation between the nature of the electrolytes and the charge of EDL at SLG electrode are relatively scarce. In our previous work, SLG was transferred onto an Au quartz and used as a two-dimensional platform to study the ion fluxes at the interface between SLG and neat ionic liquid electrolyte,[11] using EQCM and electrochemical impedance spectroscopy (EIS). In this work, the electrochemistry of SLG electrode was compared in ionic liquid electrolytes with or without the addition of acetonitrile. We reveal the ion dynamics on a polarized SLG electrode in a solvent-containing diluted organic electrolyte by using EQCM, which remarkably differs from previous results obtained from porous carbons in the similar electrolyte.[16]

Results and Discussion

The electrode preparation is shown in detail in Figure S1 in the Supporting information, as well as SLG characterizations using Raman, atomic force microscopy (AFM) and optical spectroscopy in previous work.[11] EIS measurements were performed in 2 M 1-ethyl-3-methylimidazolium bis(trifluoromethanesulfonyl)imide (EMImTFSI) diluted in acetonitrile (ACN), at various constant potential versus Ag quasi-reference electrode. As shown in Figure S2, the Nyquist plot measured at 0.2 V vs. Ref. in 2 M EMImTFSI/ACN reveals a typical capacitive behavior. The normalized real $C'(\omega)$ and imaginary $C''(\omega)$ parts of the capacitance $C(\omega)$ in the same electrolyte are shown in Figure 1a at three different potentials, in which $C'(\omega)$ corresponds to the interfacial capacitance (C_{int}) of the electrode while $C''(\omega)$ accounts for dissipative processes. The procedure of processing impedance data can

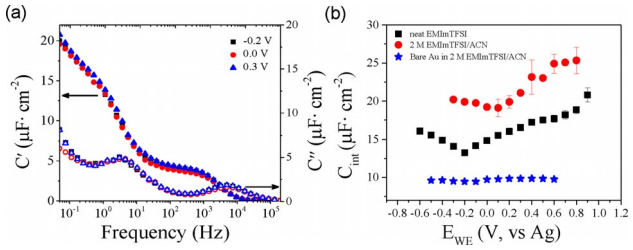

Figure 1. Capacitance change of a SLG electrode in diluted ionic liquid electrolyte. a) Real part and imaginary parts of electrochemical capacitance (C' and C'', respectively) of SLG with respect to the applied frequency, measured at different potentials in 2 M EMImTFSI/ACN. b) C_{int}-E curves of SLG in neat ionic liquid and ionic liquid dissolved in ACN electrolytes, where C_{int} is the interfacial capacitance of the SLG electrode obtained from the extrapolation.

be found in Supporting Information. Two maximal peaks are observed for $C''(\omega)$, at characteristic frequencies (f_0) of 2.48 kHz and 2.7 Hz, corresponding to time constants ($\tau_0 = 1/f_0$) of 0.4 and 370 ms, respectively. The relaxation response at 2.7 Hz is associated with the SLG/electrolyte interface, while the one at 2.48 kHz is associated with the (small area of) uncovered Au substrate. The characteristic frequency measured at 2.7 Hz is similar to that obtained for SLG electrode in neat EMImTFSI.[11]

Figure 1b shows the changes of measured C_{int} (where $C_{int} = 2C'(f_0)$ and the capacitance contribution from the uncovered Au substrate has been removed) with an applied potential in solvated EMImTFSI electrolyte, as well as in solvent-free, neat EMImTFSI, for the sake of comparison. With no surprise, results obtained in neat EMImTFSI electrolyte are similar to those reported previously.[11] The dependence of C_{int} on the ap-plied potential in 2 M EMImTFSI/ACN shows a similar V-shape behavior as in neat EMImTFSI, but with remarkably higher values in solvated ionic liquid than in pure ionic liquid. This is in line with the overscreening and crowding effects at polarized interface in neat ionic liquid, resulting in a thicker double layer and thus a decrease of interfacial capacitance in neat ionic liquids.[15b,17] Differently, the high dielectric constant of ACN (38.8) results in a decrease in the screening length,[18] and also in the double layer thickness, thus improving the overall capacitance in diluted ionic liquids.

As noticed, the pzc shifts from −0.2 V vs. Ref. to 0.1 V vs. Ref. with the addition of ACN, which is likely attributed to the change in interactions between SLG and $EMIm^+$ cations. It is worth noting that the pzc of carbide derived carbon (CDC) based electrodes was positive in the same electrolytes.[16] Besides, molecular dynamics (MD) simulations have shown the existence of strong $EMIm^+$ cation/SLG interactions due to the CH-π intermolecular interactions between alkyl side chain and SLG surface, and the π-π interaction, which results in a preferable orientation of $EMIm^+$ cation parallel onto the sur-face of negatively charged SLG.[19] With the presence of ACN solvent, the charge screening effect likely leads to a decrease of the affinity between the solvated $EMIm^+$ cations and SLG, which may account for the more positive pzc value measured. From the calculated values of interfacial capacitance from pzc to negative and positive potentials in

neat EMImTFSI and 2 M EMImTFSI/ACN (Figure 1b and Table S1), strong interaction between $EMIm^+$ and SLG was observed again. From pzc to positive polarization, where $TFSI^-$ anions are supposed to be involved as counter ions for electrode charge screening in the first approximation, the interfacial capacitance (slope of the positive branch in the plot of Figure 1b) remains nearly unchanged with the addition of solvent. However, from pzc to negative polarization, the interfacial capacitance was strongly affected by the presence of solvent, as seen from the largely reduced slope below pzc. The interfacial capacitance has been reported to be also correlated to the change of charge carriers in the graphene under polarization,[8,13,20] and the following part will be focused on the interfacial capacitance of the SLG electrode.

The capacitance at the SLG/electrolyte interface (C_{int}) can be split into the contribution of a space charge capacitance, C_{SC} and a double layer capacitance, C_{EDL} [Eq. (1)].[21]

$$1/C_{int} = 1/C_{SC} + 1/C_{EDL} \quad (1)$$

C_{SC} is further determined by parameters in the electrode material and at the interface by the Mott-Schottky equation [Eq. (2)],[22]

$$d(C_{SC}^{-2})/dE = 2/(\varepsilon\varepsilon_0 A^2 e N_D) \quad (2)$$

where A is the area, ε_0 is the permittivity of free space, ε is the dielectric constant of the electrode (typically for semiconductors), N_D is the charge carriers density, e is the electronic charge, E is the applied voltage.

Based on Equations (1) and (2), Mott-Schottky plots ($1/C_{int}^2$–E)[22] are shown in Figure 2 for SLG electrode in neat ionic liquid and solvated ionic liquid electrolytes, from pzc to negative and positive potentials. The Mott-Schottky plot for the bare (uncoated) Au electrode in the inset of Figure 2 shows the expected, typical signature of a metallic electrode with a constant double layer capacitance over the whole potential range. Interestingly, the SLG electrode exhibits a strong potential correlation with n-type and p-type semiconductor characteristics under negative and positive polarizations, respectively, in both electrolytes.[22,23] Such a difference between bare Au and SLG coated electrode supports the expectation that the capacitance is governed not only by the electronic properties of the graphene, but also by the specific organization of the electrolyte side at the SLG surface originating from the strong interactions existing between the cations and SLG surface.[7b] Thus, it is consistent with the Graham's model of the double layer,[24] which considers the presence of specifically adsorbed ions in direct contact with the electrode surface. C_{SC} can be seen, in the peculiar case of a 2D SLG electrode, as the capacitance of the SLG including a specifically adsorbed $EMIm^+$ cations layer. This is supported by the results of Figure 2, showing that the SLG/electrolyte interface follows a typical Mott-Schottky plot, whereas no variation occurs for bare Au electrode.

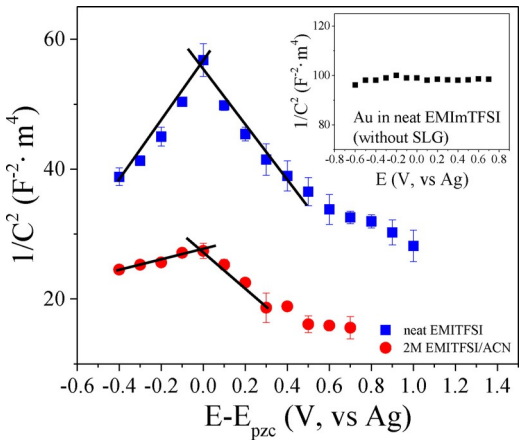

Figure 2. Mott-Schottky analysis of SLG supported on Au coated quartz in neat EMImTFSI and 2 M EMImTFSI/ACN electrolytes. The inset shows the same plot for the uncoated Au quartz in neat EMImTFSI electrolyte.

According to Mott-Schottky equation and since C_{EDL} is found out to be constant with potential (Au electrode capacitance in Figure 1), then it comes [Eq. (3)]:

$$d(C_{SC}^{-2})/dE = d(C_{int}^{-2})/dE = 2/(\varepsilon\varepsilon_0 A^2 e N_D) \quad (3)$$

The negative slope of the Mott-Schottky plot during the polarization from pzc to positive potentials well agrees with the p-doped SLG used in this study, as previously measured from Raman spectroscopy.[5] From pzc to negative potentials, the electron doping in SLG results in a change of the sign of the slope in the Mott-Schottky analysis.[9c,25] In this potential range, n-doping of SLG might be favored by the strong interaction of $EMIm^+$ and SLG, such as reported by Velpula et al.[14]

In addition, the evolution of C_{int}^{-2} respective to the potential seems sensitive to the electrolyte. As shown in Figure 2 and Table S2, the evolution of the slope of C_{int}^{-2}–E curves evidence that the addition of ACN impacts the charge carrier density at the SLG/ionic liquid interface.[14] Based on the slope and Equation (2), the charge carrier density (N_D) was calculated in the level of 10^{23} cm^{-3} for the SLG electrode immersed in neat ionic liquid, from both pzc to positive and negative polarizations. Considering a Debye length of about 1 nm in neat ionic liquid,[13] this translates into a charge carrier density $N_D \approx 10^{14}$ cm^{-2}, that is similar to the charge doping density previously reported for SLG electrode (10^{12}–10^{14} cm^{-2}).[26] For positive potentials, the slopes with (-17.7 $F^{-2}m^4V^{-1}$) or without (-25.9 $F^{-2}m^4V^{-1}$) solvent indicate a slightly higher N_D in solvated electrolyte but essentially very similar N_D level. However, from pzc to negative polarization, the slope of C^{-2}–E curve in EMImTFSI is five times higher than that in 2 M EMImTFSI/ACN. As a result, the calculated charge carrier density in 2 M EMImTFSI/ACN is one magnitude larger than neat ionic liquid. The higher charge carrier density observed for solvated electrolyte compared to neat ionic liquid, especially from pzc to negative polarization, refers to the higher charge density at the SLG/electrolyte interface. The charge screening below pzc in the solvated IL electrolyte is achieved by $EMIm^+$ cations within a shorter Debye length because of the absence of overscreening,[17] thus increasing the charge carrier density N_D.

The effect of solvent on ionic dynamics at polarized SLG has also been probed by EQCM. The SLG electrode was cycled in 2 M EMImTFSI/ACN at a scan rate of 30 mV s^{-1} from −0.65 to 1.3 V vs. Ref. as shown in the blue scatters in Figure 3a. The cyclic voltammogram (CV) shows a capacitive charging/discharging behavior. The electrochemical signals are confirmed from SLG by comparing with the CV of bare Au (Figure S3). The frequency response recorded by EQCM appears as black scatters in Figure 3a. Motional resistance was stable during polarization as shown in Figure S4. A hysteresis of EQCM frequency is observed between the positive and negative scans in one cycle. Since there is no irreversible mass change after a full cycle, as can be seen from the overlapped starting and ending points in the Δf vs. E plot, the hysteresis is assumed to originate from the difference in adsorption kinetics between cations and anions, especially near the pzc where ion exchange occurred.[27]

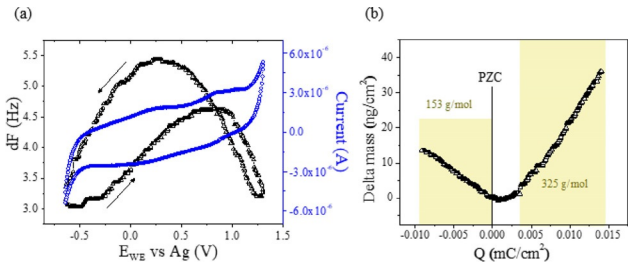

Figure 3. EQCM results of SLG in solvated ionic liquid electrolyte. a) CV and EQCM frequency response at 30 mV s^{-1} and b) electrode mass change vs. charge at 10 mV s^{-1} during the polarization of SLG on Au electrode in 2 M EMImTFSI/ACN electrolyte.

To minimize the hysteresis in the ion-mixing zone, cycling was done separately from pzc to negative or to positive potentials. Figure 3b shows the change of the electrode weight (Δm) vs. charge (ΔQ) recorded at a potential scan rate of 10 mV s^{-1}, in which the weight change is calculated from the Sauerbrey's equation [Eq. (4)].

$$\Delta m = ((-A\sqrt{u_q \rho_q})/(2 f_0^2))\Delta f = -C_f \Delta f \quad (4)$$

Figure 3b shows an increase of mass from pzc to positive and negative charges. The yellow-shaded areas show constant mass change. Using Faraday's law, the calculated molecular weight of the yellow areas is 152 and 325 g mol^{-1} during negative and positive polarization, respectively. With the theoretical molecular weight of EMIm$^+$ cation (111 g mol^{-1}), TFSI- anion (280 g mol^{-1}) and ACN solvent molecule (41 g mol^{-1}), the calculation shows that, from pzc to negative charge, each solvated EMIm$^+$ cation adsorbed on SLG takes 1 ACN molecule in average. From pzc to positive charge, the charge compensation is made by the adsorption of TFSI$^-$ anion solvated in average with 1.3 ACN molecule.

Results from EQCM experiments were further confirmed by Molecular Dynamic simulations, as shown in Figures S5 and S6. Based on the simulation, a sketch of the electrolyte organization at SLG surface is shown in Figure 4, for a typical positive/negative potential. Figures 4 and S6 show that the

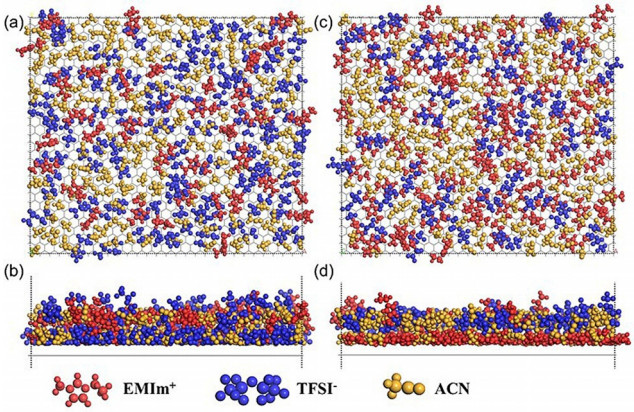

Figure 4. Top and side view of the structural model of a 2 M EMImTFSI/ACN electrolyte at SLG electrode surface, with surface charge of (a) and (b) +0.02 e/Atom, (c) and (d) −0.02 e/Atom. The atoms of Au electrode are hidden.

presence of solvent molecules in the electrolyte (compared to neat ionic liquid[11]) results in a counter-ion adsorption mechanism in the vicinity of the electrode surface under both positive and negative polarizations, in good agreement with the experimental EQCM measurements.

The counter-ion adsorption at SLG electrode in solvated EMImTFSI electrolyte is dramatically different from our previous results on SLG in neat EMImTFSI ionic liquid electrolyte,[11] in which a charged species, statistically expressed as [EMIm$_{1.58}$,TFSI$_{0.58}$]$^+$, desorbed from SLG surface during positive polarization, and ion rearrangement at the SLG surface was found to be responsible from pzc to negative potential (see Figure S7). In neat ionic liquid electrolyte, the long-range electrostatic force between charged electrode surface and ions generates a thicker double layer, that limits the ion movement.[28] The presence of solvent molecules, that screen the electrostatic interactions between cations and anions, reduces the specific EMIm$^+$ cations/SLG interactions and thus the double layer thickness, resulting in improved ionic mobility and a counter-ion adsorption on the SLG electrode surface (see Figure 3b). In contrast to the EQCM results based on three-dimensional (3D) microporous carbon electrode in 2 M EMImTFSI in ACN electrolyte, where cation adsorption occurred with about 3 to 4 solvent molecules in carbon micropores (1 nm pore size), EMIm$^+$ cation adsorption has been achieved with only 1 solvent molecule for the SLG electrode. This is surprising considering no spatial confinement is expected on such 2D electrode. The difference in the adsorption mechanism may be explained by the specific strong CH-π intermolecular and π-π interactions between EMIm+ and SLG,[19] which are less present in amorphous carbons with limited content of sp^2-hybridized carbons. These results suggest that not only the pore size and pore size distribution affect the capacitance of 3D porous carbons but also the carbon structure, the presence of sp^2 hybridized carbon resulting in stronger interaction between EMIm$^+$ cations and the SLG surface.

Conclusion

In this work, we characterized the effect of solvent addition to ionic liquid electrolyte on the electrochemical behavior of SLG electrode, using steady state and transient techniques, respectively electrochemical impedance spectroscopy (EIS) and electrochemical quartz microbalance (EQCM) coupled with cyclic voltammetry (CV) static and dynamic experiments. The electrolyte/SLG interface was characterized by EIS in solvated ionic liquid, then further analyzed by Mott-Schottky method. The screening effect due to the presence of solvent molecules significantly alters the ion interaction with the SLG, by weakening the specific interaction between $EMIm^+$ cation and SLG, leading to a rise of the charge carrier density at the electrolyte/SLG interface. Such finding points out the charge storage mechanism involves both the carbon and the electrolyte through specific interactions. On the other hand, the charge storage mechanisms of SLG in solvated ionic liquid electrolyte probed by using EQCM technique exhibits different ion responses comparing to neat ionic liquid. Differently from 3-dimmensionnal high surface area, amorphous porous carbons, counter-ion adsorption charge storage mechanism was observed on SLG during both positive and negative polarizations, which well aligns with the classic electrical double layer theory at flat, planar electrode. This suggests the importance of the local sp^2 carbon organization on its capacitive behavior and electrochemical performance.

We believe the knowledge obtained from the experimental approach developed here will be of help in designing carbon-based materials for various applications including energy storage (supercapacitors) but also capacitive deionization cell for water desalination, where counter-ion adsorption mechanism has to be favored to improve the desalination efficiency,[29] or for any application where ion fluxes in confined electrolytes plays an important role such as nanoionics.

Acknowledgements

J.L. Ye thanks the support from China Scholarship Council (CSC). K. Ni thanks the China Postdoctoral Science Foundation (2019TQ0306). G. Jiang thanks the National Natural Science Foundation of China (grant no. 21905215) for support. This work was supported by Natural Science Foundation of China (51772282, 51972299, 52003265). P. Simon and P. L. Taberna acknowledge the support from Agence Nationale de la Recherche (Labex Store-ex) and ERC Synergy Grant MoMa-Stor #951513.

Conflict of interest

The authors declare no conflict of interest.

Keywords: charge storage · electrochemical quartz crystal microbalance · electrode/electrolyte interface · graphene · supercapacitor

[1] P. Simon, Y. Gogotsi, B. Dunn, *Science* **2014**, *343*, 1210 – 1211.
[2] a) P. Simon, Y. Gogotsi, *Nat. Mater.* **2008**, *7*, 845 – 854; b) W. Gu, G. Yushin, *Wiley Interdiscip. Rev. Energy Environ.* **2014**, *3*, 424 – 473.
[3] a) Y. Zhang, L. Zhang, C. Zhou, *Acc. Chem. Res.* **2013**, *46*, 2329 – 2339; b) E. McCann, M. Koshino, *Rep. Prog. Phys.* **2013**, *76*, 056503; c) Y. Zhu, S. Murali, W. Cai, X. Li, J. W. Suk, J. R. Potts, R. S. Ruoff, *Adv. Mater.* **2010**, *22*, 3906 – 3924.
[4] M. F. El-Kady, Y. Shao, R. B. Kaner, *Nat. Rev. Mater.* **2016**, *1*, 16033.
[5] J. Ye, H. Tan, S. Wu, K. Ni, F. Pan, J. Liu, Z. Tao, Y. Qu, H. Ji, P. Simon, Y. Zhu, *Adv. Mater.* **2018**, *30*, 1801384.
[6] J. Ye, P. Simon, Y. Zhu, *Natl. Sci. Rev.* **2020**, *7*, 191 – 201.
[7] a) J. Xia, F. Chen, J. Li, N. Tao, *Nat. Nanotechnol.* **2009**, *4*, 505 – 509; b) M. D. Stoller, C. W. Magnuson, Y. Zhu, S. Murali, J. W. Suk, R. Piner, R. S. Ruoff, *Energy Environ. Sci.* **2011**, *4*, 4685; c) A. A. Kornyshev, N. B. Luque, W. Schmickler, *J. Solid State Electrochem.* **2014**, *18*, 1345 – 1349.
[8] J.-H. Zhong, J.-Y. Liu, Q. Li, M.-G. Li, Z.-C. Zeng, S. Hu, D.-Y. Wu, W. Cai, B. Ren, *Electrochim. Acta* **2013**, *110*, 754 – 761.
[9] a) C. Zhan, J. Neal, J. Wu, D.-e. Jiang, *J. Phys. Chem. C* **2015**, *119*, 22297 – 22303; b) E. Uesugi, H. Goto, R. Eguchi, A. Fujiwara, Y. Kubozono, *Sci. Rep.* **2013**, *3*, 1595; c) H. X. Ji, X. Zhao, Z. H. Qiao, J. Jung, Y. W. Zhu, Y. L. Lu, L. L. Zhang, A. H. MacDonald, R. S. Ruoff, *Nat. Commun.* **2014**, *5*, 3317.
[10] a) M. Jitvisate, J. R. T. Seddon, *J. Phys. Chem. Lett.* **2018**, *9*, 126 – 131; b) Z. A. H. Goodwin, G. Feng, A. A. Kornyshev, *Electrochim. Acta* **2017**, *225*, 190 – 197; c) Z. A. Goodwin, A. A. Kornyshev, *Electrochem. Commun.* **2017**, *82*, 129 – 133.
[11] J. Ye, W. Yih-Chyng, K. Xu, K. Ni, N. Shu, P.-L. Taberna, Y. Zhu, P. Simon, *J. Am. Chem. Soc.* **2019**, *141*, 16559 – 16563.
[12] a) P. Sharma, Z. L. Mišković, *Phys. Rev. B* **2014**, *90*, 125415; b) L. Daniels, M. Scott, Z. L. Mišković, *J. Chem. Phys.* **2017**, *146*, 094101; c) X. Du, H. Guo, Y. Jin, Q. Jin, J. Zhao, *Electroanalysis* **2015**, *27*, 2760 – 2765; d) Y. Han, S. Huang, T. Yan, *J. Phys. Condens. Matter* **2014**, *26*, 284103; e) L. Yin, Y. Huang, H. Chen, T. Yan, *Phys. Chem. Chem. Phys.* **2018**, *20*, 17606 – 17614.
[13] A. Shalabi, L. Daniels, M. Scott, Z. L. Mišković, *Electrochim. Acta* **2019**, *319*, 423 – 434.
[14] G. Velpula, R. Phillipson, J. X. Lian, D. Cornil, P. Walke, K. Verguts, S. Brems, H. Uji-i, S. De Gendt, D. Beljonne, R. Lazzaroni, K. S. Mali, S. De Feyter, *ACS Nano* **2019**, *13*, 3512 – 3521.
[15] a) A. A. Kornyshev, E. Spohr, M. A. Vorotyntsev, *Encycl. Electrochem.* **2007**, 9783527302505; b) M. V. Fedorov, A. A. Kornyshev, *Chem. Rev.* **2014**, *114*, 2978 – 3036; c) D. Weingarth, M. Zeiger, N. Jäckel, M. Aslan, G. Feng, V. Presser, *Adv. Energy Mater.* **2014**, *4*, 1400316.
[16] W.-Y. Tsai, P.-L. Taberna, P. Simon, *J. Am. Chem. Soc.* **2014**, *136*, 8722 – 8728.
[17] M. Z. Bazant, B. D. Storey, A. A. Kornyshev, *Phys. Rev. Lett.* **2011**, *106*, 046102.
[18] A. A. Lee, C. S. Perez-Martinez, A. M. Smith, S. Perkin, *Faraday Discuss.* **2017**, *199*, 239 – 259.
[19] a) E. Paek, A. J. Pak, G. S. Hwang, *J. Electrochem. Soc.* **2013**, *160*, A1 – A10; b) M. Vijayakumar, B. Schwenzer, V. Shutthanandan, J. Hu, J. Liu, I. A. Aksay, *Nano Energy* **2014**, *3*, 152 – 158; c) S. Maolin, Z. Fuchun, W. Guozhong, F. Haiping, W. Chunlei, C. Shimou, Z. Yi, H. Jun, *J. Chem. Phys.* **2008**, *128*, 134504.
[20] V. Lockett, M. Horne, R. Sedev, T. Rodopoulos, J. Ralston, *Phys. Chem. Chem. Phys.* **2010**, *12*, 12499 – 12512.
[21] A. Hankin, F. E. Bedoya-Lora, J. C. Alexander, A. Regoutz, G. H. Kelsall, *J. Mater. Chem. A* **2019**, *7*, 26162 – 26176.
[22] P. Knauth, Y. Massiani, *J. Electroanal. Chem.* **1998**, *442*, 229 – 234.

[23] K. Gelderman, L. Lee, S. W. Donne, *J. Chem. Educ.* **2007**, *84*, 685.
[24] D. C. Grahame, *Chem. Rev.* **1947**, *41*, 441 – 501.
[25] H. Gerischer, R. McIntyre, D. Scherson, W. Storck, *J. Phys. Chem.* **1987**, *91*, 1930 – 1935.
[26] a) G. Sarau, M. Heilmann, M. Bashouti, M. Latzel, C. Tessarek, S. Christiansen, *ACS Appl. Mater. Interfaces* **2017**, *9*, 10003 – 10011; b) S. Y. Shin, N. D. Kim, J. G. Kim, K. S. Kim, D. Y. Noh, K. S. Kim, J. W. Chung, *Appl. Phys. Lett.* **2011**, *99*, 082110.
[27] a) M. D. Levi, S. Sigalov, G. Salitra, D. Aurbach, J. Maier, *ChemPhysChem* **2011**, *12*, 854 – 862; b) Y.-C. Wu, P.-L. Taberna, P. Simon, *Electrochem. Commun.* **2018**, *93*, 119 – 122.
[28] M. A. Gebbie, A. M. Smith, H. A. Dobbs, G. G. Warr, X. Banquy, M. Valtiner, M. W. Rutland, J. N. Israelachvili, S. Perkin, R. Atkin, *Chem. Commun.* **2017**, *53*, 1214 – 1224.
[29] a) M. E. Suss, S. Porada, X. Sun, P. M. Biesheuvel, J. Yoon, V. Presser, *Energy Environ. Sci.* **2015**, *8*, 2296 – 2319; b) P. Srimuk, X. Su, J. Yoon, D. Aurbach, V. Presser, *Nat. Rev. Mater.* **2020**, *5*, 517.

Manuscript received: December 23, 2020
Accepted manuscript online: February 8, 2021
Version of record online: March 11, 2021

